Polymer Journal (2022) 54:735–740
https://doi.org/10.1038/s41428-022-00619-x

NOTE

Direct synthesis of a robust cellulosic composite from cellulose acetate and a nanofibrillated bacterial cellulose sol

Naoki Wada[1] · Tetsuo Fujie[1] · Ren Sasaki[1] · Tokuo Matsushima[2] · Kenji Takahashi[1]

Received: 30 November 2021 / Revised: 20 December 2021 / Accepted: 6 January 2022 / Published online: 22 February 2022

Abstract

Cellulose nanofibers (CNFs) are potential candidates as environmentally friendly reinforcing fibers, and their compatibilization with plastics has attracted widespread interest. In this study, we developed a simple method to prepare a cellulose acetate (CA) composite reinforced by nanofibrillated bacterial cellulose (NFBC) directly from an aqueous sol. The key steps of our method were the utilization of a water/organic mixed solvent to maintain a good dispersion of the NFBC and good dissolution of CA, along with the evaporation of this mixed solvent without significant aggregation of the NFBC. This simple technique improved the dispersibility of the NFBC in the composite film and significantly enhanced its mechanical strength.

Introduction

Cellulose nanofibers (CNFs) are expected to be among the next generation of reinforcing fibers [1] because of their unique characteristics, such as carbon neutrality, biodegradability in nature, high mechanical performance [2], low weight, chemical modification capability, high net electrical dipole moment [3], and recyclability. Their easy chemical modification facilitates compatibilization with various types of resin. To enhance reinforcement, CNFs can be aligned in one direction by an electric and/or magnetic field, owing to their high net electrical dipole moment [4]. Moreover, fiber breakage during kneading can be minimized under optimized conditions [5], leading to negligible performance degradation during repeated use.

CNFs can be classified into two categories based on their production processes: top-down [6] and bottom-up [7]. Mechanically and/or chemically defibrated plant-based pulp (crystal-type I_β) can be used to produce CNFs. CNFs are generally obtained as an aqueous dispersion (sol), and their morphology, fiber length and width, and physicochemical properties vary depending on the defibration method. Once water is evaporated by heating or freeze-drying, severe aggregation of CNFs occurs. Generally, redispersion is difficult because of the multiple hydrogen bonds between the CNF surfaces; consequently, the interfacial shear stress between the matrix resin and CNF surface becomes uncontrollable. It is necessary to develop a technology to prevent CNF agglomeration during the synthesis of fiber-reinforced plastics (FRPs). TEMPO-oxidized CNFs were developed by Isogai et al. to maintain high dispersibility in water. Electrostatic repulsion is very effective in producing completely nanodispersed transparent CNF sols [8, 9]. Such a CNF sol is highly compatible with water-soluble polymers, such as PVA [10], and nanocomposites with hydrophobic polymers can also be produced via emulsion polymerization. Yano et al. reported that the esterification of hydroxyl groups with fatty acyl chains aided the dispersion of CNFs in high-density polyethylene (HDPE), resulting in approximately twice the tensile strength of the base resin [11].

CNFs can also be produced via fermentation by microbes, such as gluconacetobacter. Such CNFs are hereafter referred to as bacterial cellulose nanofibers (BCNFs) in this study. The cellulose purity is high, as hemicellulose and lignin are not produced; thus, the crystallinity of BCNFs is sufficiently higher (~96%) than that of pulp-derived CNFs [12]. Furthermore, BCNFs have type I_α crystals and are as strong as pulp-derived

Supplementary information The online version contains supplementary material available at https://doi.org/10.1038/s41428-022-00619-x.

✉ Naoki Wada
naoki-wada@se.kanazawa-u.ac.jp

✉ Kenji Takahashi
ktkenji@staff.kanazawa-u.ac.jp

[1] Faculty of Biological Science and Technology, Institute of Science and Engineering, Kanazawa University, Kakuma-machi, Kanazawa, Japan

[2] Kusano Sakko Inc., Nishi-machi, Kami-ebetsu, Ebetsu, Japan

fibers [13, 14]. However, BCNFs are generally produced as hydrogel mats on the surface of fermentation media [15]; therefore, dispersion in water or an organic solvent is essential for their utilization as reinforcing fibers. In 2017, Tajima et al. reported that well-dispersed BCNFs in the medium were obtained when several types of water-soluble cellulosic polymers were added to the culture medium [16]. These are referred to as nanofibrillated bacterial cellulose (NFBC) to distinguish it from mat-shaped BCNFs. The NFBC fibers are extremely long. Therefore, they can be expected to become entangled with each other in the polymer matrix, thereby strengthening the composite material, even at a low loading percentage. The NFBCs could also be dispersed in several types of water-miscible organic solvents; consequently, a better compatibility with the resin matrix can be expected compared to other CNFs. Although the fabrication of transparent composite films comprising NFBCs and polymethyl methacrylate (PMMA) was successful, the mechanical strength enhancement was insufficient [16]. An aminopropylsilylated NFBC (AP-NFBC) was recently developed, and PMMA was strengthened by more than two times by adding only 1 wt% AP-NFBC [17].

Recently, microplastic pollution in oceans caused by nonbiodegradable petroleum plastics has emerged as a serious concern. The replacement of these plastics with biodegradable and biomass-derived alternatives is being actively pursued. Hence, bioplastics will become a particularly important matrix resin for FRPs in the near future. Currently, ~2.5 million tons of biomass plastics are produced annually, with cellulose acetate (CA) accounting for the largest proportion (0.8 million tons). Cellulosic resin is expected to become the most versatile resin in the near future, as cellulose is the most abundant carbon source polymer on earth. Furthermore, the ester and glycosidic bonds in cellulose ester resin can be enzymatically or chemically digested to generate a monomeric unit, glucose. Because of the (bio)chemical recyclability of both cellulose esters and CNFs, CNF-reinforced cellulose ester resin, which is an all-cellulosic composite, is a promising green material. Based on these social and technological backgrounds, this study focuses on cellulosic composites. In this study, two processes, one dry and one wet, were investigated for compositing CA and NFBCs. We found that the wet process worked notably well to avoid NFBC aggregation in the CA matrix, providing a robust composite material.

Experimental procedure

General

NFBC sols modified with water-soluble cellulose ethers, such as carboxymethyl, hydroxypropyl, and hydroxyethyl cellulose (abbreviated as CM-, HP-, and HE-NFBC, respectively), were procured from Kusano Sakko Co. (Hokkaido, Japan). CA was donated by DSP Gokyo Food and Chemical Co. (Osaka, Japan) in the form of pellets. CA was soluble in acetone and was thus classified as cellulose diacetate. The compatibilization of CA and the three NFBCs was performed using two methods: dry and wet processes.

Dry process for preparing the NFBC/CA composite

The NFBC sol was freeze-dried to obtain a dry NFBC solid. Predetermined weights of the dry NFBC were crushed by hand to be smaller than the injection port (∅: 0.8 mm) of an extruder. This crushed NFBC and CA were kneaded in the extruder at 190 °C with a screw speed of 60 rpm for up to 20 min to produce composite pellets.

Wet process for preparing the NFBC/CA composite

The NFBC concentration in the hydrosol was adjusted to a predetermined value, such that the weight ratio of the dry NFBC to dry CA (NFBC/CA) ranged from 1/99 to 10/90. Acetone (250 mL) was added to the NFBC sol (50 g), and the mixture was stirred for at least 1 h until the NFBCs were uniformly dispersed. CA pellets (4.5 g) were added to the mixture and dissolved completely. Ultraviolet–visible (UV–vis) absorption spectra were measured with a V-630 (JASCO, Tokyo, Japan) to confirm negligible aggregation of NFBCs. The resulting mixture was poured into a stainless-steel bat, and the solvent was evaporated at room temperature (air-conditioned at 25 °C) under ambient pressure. The resulting cast film was cut into small pieces and dried under reduced pressure. The raw film was kneaded at 190 °C with a screw speed of 60 rpm for 5 min to obtain the composite pellets.

Preparation of the specimen for the mechanical test

The composite material was kneaded and pelletized to obtain a uniform FRP. The kneaded composite pellet was preheated at 190 °C for 5 min and then hot-pressed at 40 kN (1.56 MPa) for 3 min to form a film. The dumbbell-shaped specimen was prepared in accordance with the JIS K7139 method. The tensile test was conducted using an EZ-SX (Shimadzu Co, Kyoto, Japan), and the mechanical properties were analyzed using Trapezium X software.

Results and discussion

NFBC/CA composite prepared by the dry process

When the dry CM-NFBC was kneaded directly with CA, there was no change in the elastic modulus. The tensile

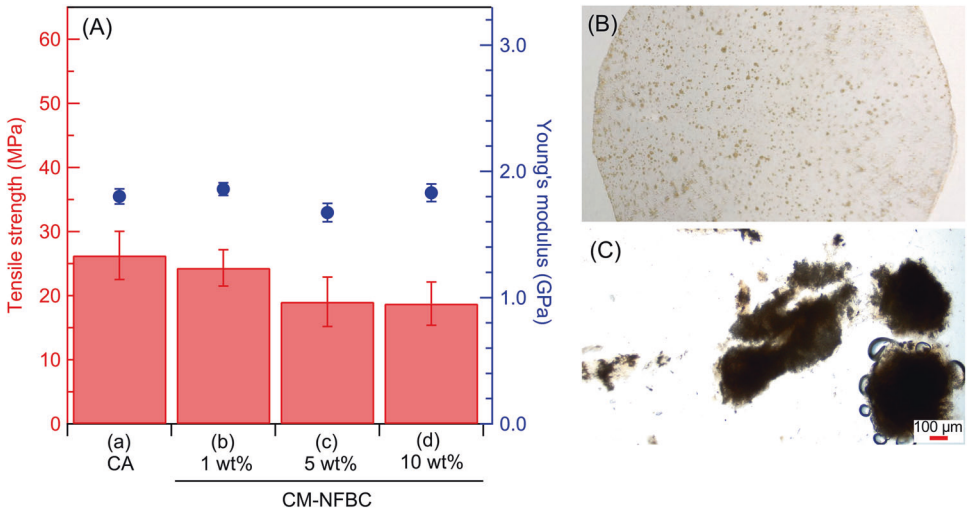

Fig. 1 (**A**) Tensile strength and Young's modulus of the CM-NFBC/CA composite material prepared by the dry process. (**B**) Appearance and (**C**) optical micrograph of the hot-pressed film consisting of 5 wt% CM-NFBC

strength gradually decreased as the weight fraction of CM-NFBC increased to 5 wt% (Fig. 1A, stress–strain curves in Fig. S1). There was no significant difference in strength between the 5 and 10 wt% CM-NFBC fractions. Even with a sufficiently long kneading time of up to 20 min, CM-NFBC aggregates with a maximum diameter of ~500 μm were observed (Fig. 1B, C). The size of the aggregates could be reduced to approximately 100 μm by repeated kneading; however, the mechanical strength could not be improved. Thus, even if the NFBC surface was modified with carboxymethyl cellulose for improved hydrophobicity and electrorepulsion, once the nanofibers were agglomerated during drying, it was impossible to redisperse the nanofibers finely into the resin by kneading. Air bubbles, which may have been present in the NFBC aggregates initially, were also observed in the composite films. These bubbles could not be removed by thorough kneading, and the resulting voids were one of the reasons for the decrease in the mechanical strength.

NFBC/CA composite prepared by the wet process

CM-NFBC was well dispersed even when the CM-NFBC aqueous sol was diluted with a five times larger volume of acetone. CA was dissolved in this acetone-rich aqueous solution. The NFBC dispersion was examined by UV–vis absorption spectroscopy, and the absorbance did not obviously increase (Fig. S2). The mixture was slowly dried under ambient conditions to obtain a cloudy-white composite film. This film was kneaded and pelletized, and the pellets were hot-pressed. A visually agglomerate-free film was obtained even at a high weight fraction of CM-NFBC (Fig. 2B). Microscopic observation revealed small NFBC aggregates (Fig. 2C), but their sizes were apparently reduced compared to those in the dry process. Composite films were prepared by varying the CM-NFBC loading ratio up to 10 wt%, and a mechanical test was conducted (Fig. 2A). The tensile strength and elastic modulus of the base resin CA were 26 MPa and 1.8 GPa, respectively, which were then increased to 42 MPa and 2.4 GPa, respectively, with only 1 wt% NFBC reinforcement. A composite with 5 wt% NFBC resulted in a maximum strength and modulus of 54 MPa and 3 GPa, respectively. These are 2.1 and 1.7 times higher than those of the base resin, respectively. No significant difference in the mechanical properties was observed between the 5 and 10 wt% compositions. Optical microscopy images of the composite films are shown in Fig. S3. As the NFBC concentration increases, the number of small aggregates tends to increase, which may be one of the reasons why the mechanical properties did not continue to further improve at high NFBC loading. It is important to ensure that the NFBCs are well dispersed and CA is well dissolved in the water/organic mixed solvent and that the evaporation of this mixed solvent occurs without significant NFBC aggregation. The glass transition temperature of the CA matrix was the same regardless of the presence of NFBCs (Fig. S4). We investigated different drying methods: drying under reduced pressure, drying at a high temperature, and slow evaporation by covering with a top. All these drying methods could enhance the mechanical strength. We also evaluated different water-miscible solvents, such as dimethylformamide, N-methyl pyrrolidone, tetrahydrofuran, and dioxane, for the wet process. All these solvents were found to be effective in enhancing the mechanical properties of the composites.

The stress–strain curves of the CM-NFBC-reinforced CA composite films are shown in Fig. 3. As the CM-NFBC content increased, the tensile strength and modulus increased, although the strain decreased. The samples with 10 wt% CM-NFBC fractured in the lowest strain region.

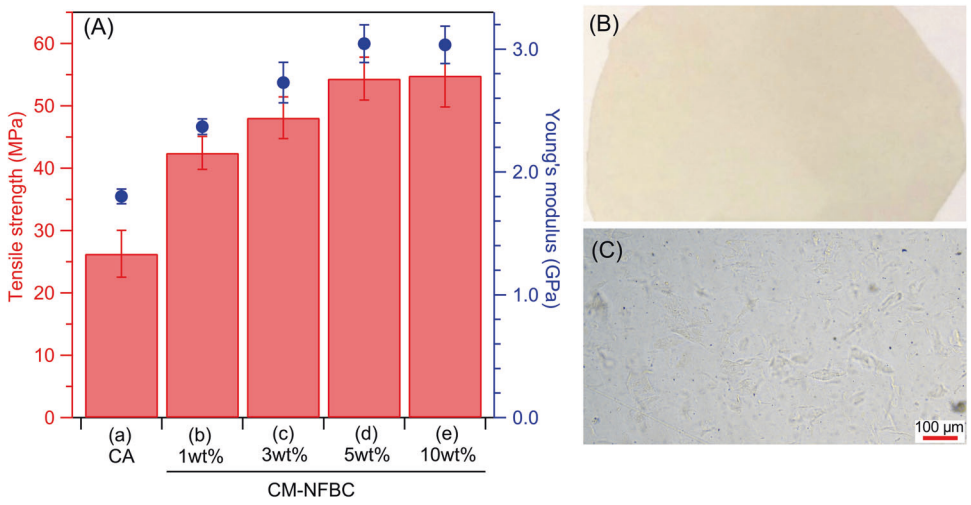

Fig. 2 (**A**) Tensile strength and Young's modulus of the CM-NFBC/CA composite material prepared by the wet process. (**B**) Appearance and (**C**) optical micrograph of the hot-pressed film consisting of 5 wt% CM-NFBC

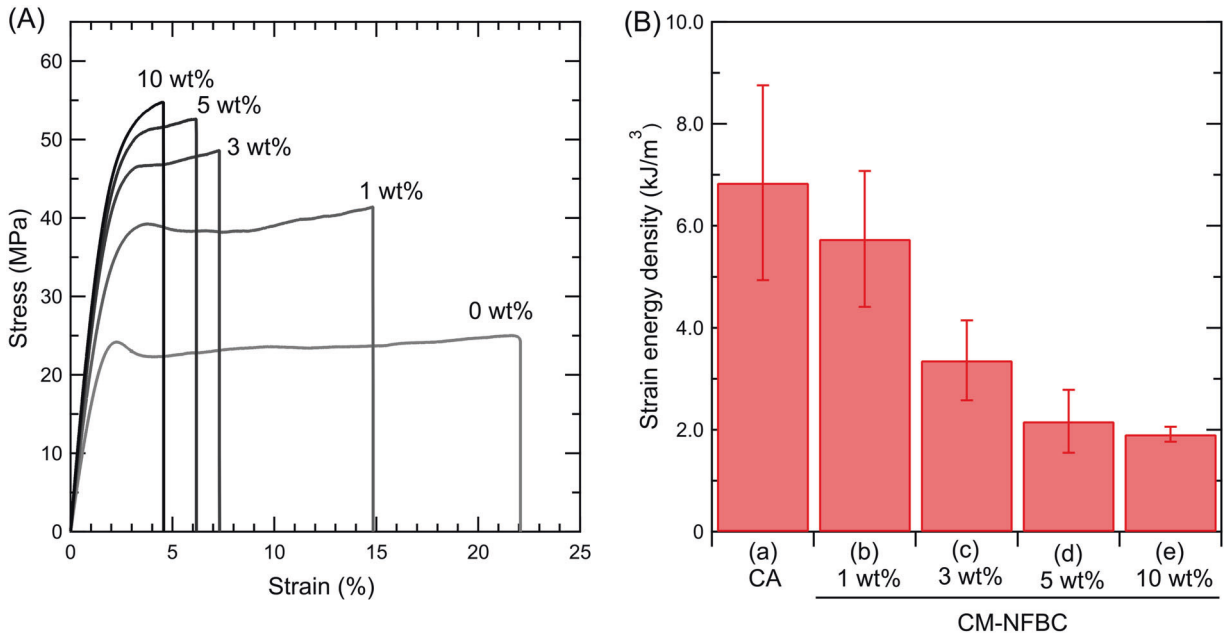

Fig. 3 (**A**) Stress–strain curve and (**B**) strain energy density of the CM-NFBC/CA composite specimen

The energy required to break the specimen, i.e., the strain energy per unit volume, decreased as the CM-NFBC content increased up to 5 wt%. However, these are typical behaviors often observed in FRPs.

Applying the wet process to other NFBCs

NFBCs modified with different water-soluble cellulose ethers, such as HP- and HE-NFBC, were also compatibilized with CA via the wet process described above. The tensile strength and elastic modulus of each composite were much higher than those of the base resin but slightly lower than those of the CM-NFBC composite (Fig. 4, stress–strain curves in Fig. S5). This result can be attributed to the difference in the interfacial shear strength between the CA matrix and the NFBC. Both CM-NFBC and CA have hydrogen bond donors and acceptors (namely, hydroxyl and carbonyl groups, respectively) in a single molecule, whereas HP- and HE-NFBC have only a hydrogen bond donor (i.e., a hydroxyl group). Therefore, CM-NFBC can be expected to have stronger interactions with the CA matrix than HP- or HE-NFBC. However, different reasons can also be speculated. Tajima et al. reported that the amount of cellulose ether adsorbed on the NFBC surface increased in the order of CM-NFBC < HE-NFBC < HP-NFBC [16]. This result indicates that the weight ratio of the native CNFs

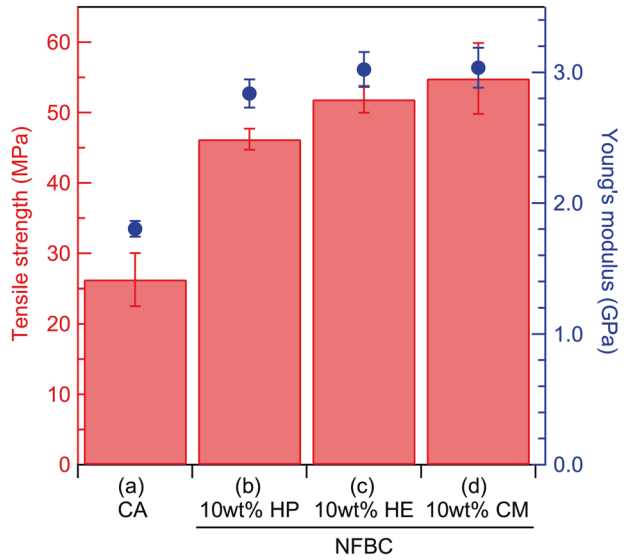

Fig. 4 Tensile strength and Young's modulus of pure CA films and those reinforced by three different kinds of NFBCs

decreased in the order of CM-NFBC > HE-NFBC > HP-NFBC, which is the same as that observed for the tensile strength of the CA/NFBC materials. Thus, the actual content of the reinforcing nanofibers can also be attributed to the mechanical strength.

Conclusions

In this study, two processes, dry and wet, were investigated for compositing CA and NFBCs. We evaluated the dispersibility of NFBCs and mechanical properties of the composite films. Once the NFBCs aggregated during water evaporation, it was impossible to redisperse the nanofibers finely into the CA matrix, even by repeated kneading. In contrast, the NFBCs were highly dispersible in a mixture of water and acetone. After dissolving CA into this NFBC organic/water sol, solvent evaporation could maintain the dispersibility of NFBCs in the CA matrix. By adding only 5 wt% NFBCs, the mechanical strength of the prepared composites became twice that of CA. The method employed herein can be regarded as a straightforward and perhaps energy-saving method for fabricating robust composites, as it does not involve any chemical modification typically required for the synthesis of wood-derived cellulose nanofiber composites. Mechanical, chemical, and biochemical recycling of the all-cellulosic composites obtained in this study will be investigated in the near future.

Acknowledgements A part of this work was supported by Grant-in-Aid for the Japan Society for the Promotion of Science (JSPS) KAKENHI Grant No. 18H02253 to KT and Grant No. 21K05704 to NW.

Compliance with ethical standards

Conflict of interest The authors declare no competing interests.

Publisher's note Springer Nature remains neutral with regard to jurisdictional claims in published maps and institutional affiliations.

References

1. Trache D, Tarchoun AF, Derradji M, Hamidon TS, Masruchin N, Brosse N, et al. Nanocellulose: from fundamentals to advanced applications. Front Chem. 2020;8:392.
2. Cheng Q, Wang S. A method for testing the elastic modulus of single cellulose fibrils via atomic force microscopy. Compos A. 2008;39:1838–43.
3. Frka-Petesic B, Jean B, Heux L. First experimental evidence of a giant permanent electric-dipole moment in cellulose nanocrystals. Europhys Lett. 2014;107:28006.
4. Li K, Clarkson CM, Wang L, Liu Y, Lamm M, Pang Z, et al. Alignment of cellulose nanofibers: harnessing nanoscale properties to macroscale benefits. ACS Nano. 2021;15:3646–73.
5. Leão RM, Luz SM, Araújo JA, Christoforo AL. The recycling of sugarcane fiber/polypropylene composites. Mater Res. 2015;18:690–7.
6. Abdul Khalil HPS, Davoudpour Y, Islam MN, Mustapha A, Sudesh K, Dungani R, et al. Production and modification of nanofibrillated cellulose using various mechanical processes: a review. Carbohyd Polym. 2014;99:649–65.
7. Lynd LR, Weimer PJ, Zyl WH, Pretorius IS. Microbial cellulose utilization: Fundamentals and biotechnology. Microbiol Mol Biol Rev. 2002;66:506–77.
8. Okita Y, Saito T, Isogai A. Entire surface oxidation of various cellulose microfibrils by TEMPO-mediated oxidation. Biomacromolecules. 2010;11:1696–700.
9. Isogai A, Saito T, Fukuzumi H. TEMPO-oxidized cellulose nanofibers. Nanoscale. 2011;3:71–85.
10. Endo R, Saito T, Isogai A. TEMPO-oxidized cellulose nanofibril/poly(vinyl alcohol) composite drawn fibers. Polymer. 2013;54:935–41.
11. Yano H, Omura H, Honma Y, Okumura H, Sano H, Nakatsubo F. Designing cellulose nanofiber surface for high density polyethylene reinforcement. Cellulose. 2018;25:3351–62.
12. Park S, Baker JO, Himmel ME, Parilla PA, Johnson DK. Cellulose crystallinity index: measurement techniques and their impact on interpreting cellulase performance. Biotechnol Biofuels. 2010;3:10.
13. Guhados G, Wan W, Hutter JL. Measurement of the elastic modulus of single bacterial cellulose fibers using atomic force microscopy. Langmuir. 2005;21:6642–46.

14. Hsieh YC, Yano H, Nogi M, Eichhorn SJ. An estimation of the Young's modulus of bacterial cellulose filaments. Cellulose. 2008;15:507–13.
15. Wang J, Tavakoli J, Tang Y. Bacterial cellulose production, properties and applications with different culture methods—a review. Carbohyd Polym. 2019;219:63–76.
16. Tajima K, Kusumoto R, Kose R, Kono H, Matsushima T, Isono T, et al. One-step production of amphiphilic nanofibrillated cellulose using a cellulose-producing bacterium. Biomacromolecules. 2017;18:3432–8.
17. Kono H, Uno T, Tsujisaki H, Matsushima T, Tajima K. Nanofibrillated bacterial cellulose modified with (3-aminopropyl)trimethoxysilane under aqueous conditions: Applications to poly (methyl methacrylate) fiber-reinforced nanocomposites. ACS Omega. 2020;5:29561–9.